H-Mat Hydrogen Compatibility of Polymers and Elastomers

Simmons, K.L.[1], Kuang, W.[1], Burton, S.D.[1], Arey, B.W.[1], Shin, Y.[1], Menon, N.C.[2], and Smith, D.B.[3]

[1] Pacific Northwest National Laboratory, PO Box 999, Richland, WA 99354, USA, kl.simmons@pnnl.gov
[2] Sandia National Laboratories, 7011 East Avenue, Livermore, CA 95391, USA, ncmenon@sandia.gov
[3] Oak Ridge National Laboratory, PO Box 2008, Oak Ridge, TN 37831, USA, smithdb@ornl.gov

ABSTRACT
The H2@Scale program of the U.S. Department of Energy (DOE) Fuel Cell Technologies Office is supporting work on the hydrogen compatibility of polymers to improve the durability and reliability of materials for hydrogen infrastructure. The hydrogen compatibility program (H-Mat) seeks "to address the challenges of hydrogen degradation by elucidating the mechanisms of hydrogen-materials interactions with the goal of providing science-based strategies to design materials, (micro)structures, and morphology with improved resistance to hydrogen degradation." This research has found hydrogen and pressure interactions with model rubber-material compounds demonstrating volume change and compression-set differences in the materials. The research leverages state-of-the-art capabilities of the DOE national labs. The materials were investigated using helium-ion microscopy, which revealed significant morphological changes in the plasticizer-incorporating compounds after exposure, as evidenced by time-of-flight secondary ion mass spectrometry. Additional studies using transmission electron microscopy and nuclear magnetic resonance revealed that nanosized inclusions developed after gas decompression in rubber- and plasticizer-only materials; this is an indication of void formation at the nanometer level.

1.0 INTRODUCTION

With the demand to reduce dependence on fossil fuels, interest has increasingly grown worldwide in clean energy carriers for both mobile applications and stationary power supplies. [1,2] Hydrogen, an abundant and environmentally friendly source of energy, will likely be used more and more frequently in the coming decade for several purposes. The United States Department of Energy's Fuel Cell Technologies Office has initiated an H2@Scale program to expand the use of hydrogen as another energy carrier to support the electrical infrastructure and industry. However, the broad use of hydrogen is currently constrained by its potential incompatibility with materials when they are exposed for long periods of time at high pressure. [3,4] Effects of high pressure on materials performance must be tested on materials associated with current hydrogen energy technologies in delivery and distribution, fueling stations, and automotive fueling systems. Specifically, under certain conditions, many metals, like some steels and titanium, have been demonstrated to be susceptible to a high-pressure hydrogen environment, which causes embrittlement and structural damage due to the formation of hydrides. [5-8] In contrast to metals, polymers are commonly considered chemically inert to hydrogen; any damage primarily results from mechanical failure. It is widely accepted in the hydrogen energy community that most damage to polymers in hydrogen applications occurs during sudden decompression of high-pressure hydrogen. This type of damage is commonly referred to as explosive decompression failure (XDF) [9,10]; it has been investigated in several studies due to growing interest in high-pressure hydrogen applications. Mechanistically, the hydrogen absorbed within the polymer matrix undergoes sudden expansion during the rapid removal of external pressure, which engenders bubbles, surface blistering, or even catastrophic failure by exfoliation.

Koga et al. [11] employed a high-pressure durability tester to investigate the high-pressure hydrogen effects on rubber O-rings. Optical micrographs of post-exposure O-rings indicated that the mechanical damage was due to surface and inner cracks. Fujiwara et al. [12] reported on filled acrylonitrile butadiene rubber (NBR) materials that are cyclically exposed to 90 MPa hydrogen gas. They found that the mechanical properties of the materials weakened due to the declining filler-polymer interaction rather than any chemical change in structure such as hydrogenation, isomerization, or chain scission. Along this line, Ohayma et al. [13] suggested that the inhomogeneity of NBR rubber microstructure could be the origin of XDF, as supported by their transmission electron microscopy (TEM) and small-angle x-ray scattering results.

Preliminary experiments were performed on several common commercial rubber materials at Sandia National Laboratories (SNL), including ethylene propylene diene (EPDM), NBR, and Viton A (all three purchased from McMaster-Carr). These materials were subjected to single-cycle 90 MPa hydrogen exposure and subsequently imaged using x-ray computed tomography. Voids had formed around fillers upon high-pressure hydrogen exposure, as shown in Figure 1. Viton A had some cracks propagating and reaching the outer surface of the sample. However, fundamental understanding of why failure modes are so different between polymers is lacking at present.

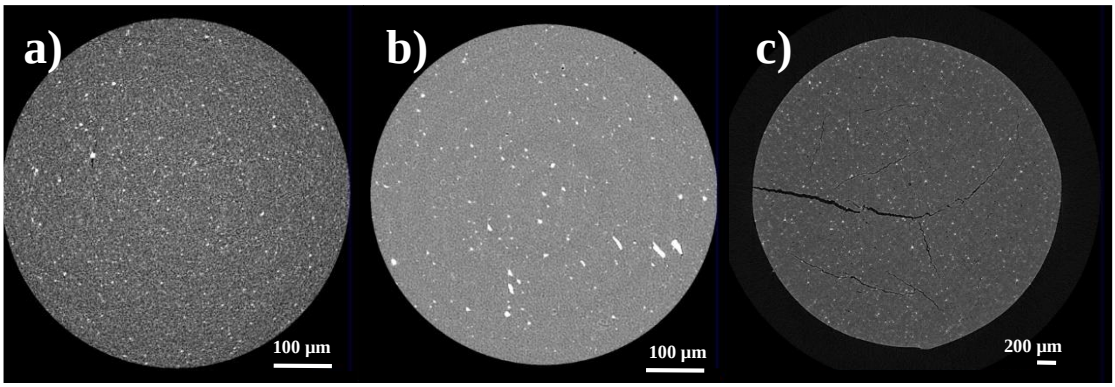

Figure 1. X-ray CT images of commercial rubber materials after 90 MPa hydrogen exposure: (a) EPDM, (b) NBR, and (c) Viton A

In this work, the high-pressure hydrogen effects on model rubber compounds (i.e., NBR compounds) are experimentally investigated, leveraging state-of-the-art capabilities of the U.S. Department of Energy (DOE) national laboratories. Such model rubber compounds contain plasticizer (i.e., dioctyl sebacate [DOS]) and/or fillers (i.e., carbon black and silica) so as to mimic the composition and performance of commercial rubber materials. Compression set and volume change of the compounds were first studied to examine effects of high-pressure hydrogen from a macroscopic perspective. Advanced morphological characterization techniques such as helium-ion microscopy (HeIM), TEM, and time-of-flight secondary ion mass spectrometry (TOF-SIMS) were adopted to evaluate and comprehend the influences of high-pressure hydrogen at the molecular level.

2.0 MATERIALS AND METHODS

2.1 Model materials

A series of six NBR model compounds was developed for this research. The work reported here focuses on two NBR compounds, as specified in Table 1. The materials were purchased from Takaishi Industry Co., Ltd. Osaka, Japan. The compound formulation N2 is a vulcanized NBR elastomer with a DOS plasticizer and no carbon black or silica filler. NBR compound N5 is a vulcanized NBR elastomer with the same quantity of DOS plasticizer as well as silica and carbon black fillers. Compound N5 simulates a commercial compound with a durometer Shore hardness of 68 A, while N2 has an expected hardness of 47 A. The materials were supplied in 15 cm × 15 cm × 0.3 cm plaques.

2.2 Experimental test setup

The pressure vessel was purged with argon before any hydrogen tests were performed for safety reasons. High-pressure hydrogen exposure was conducted using 99.99% hydrogen gas with pressures up to 90 MPa in a pressure vessel. A 22.2 mm diameter disk with a thickness of 2.9 mm was cut from each of the vulcanized plaques. Depending on the experiment, samples were exposed to various pressures from 27.6–90 MPa at an approximate flow rate of 2.1 MPa/min. The system was held isostatic for 16 h to ensure that specimens were fully saturated with hydrogen and that the temperature reached equilibrium. A second filling was done to replenish the vessel to make up pressure lost due to the adiabatic cooling of the hydrogen gas during the initial filling. The high-pressure hydrogen gas was then released at a depressurization rate of more than 0.34 MPa/min. After the exposure experiment was complete, the vessel was flushed with argon to eliminate residual hydrogen.

Table 1. NBR compound composition.

Composition (parts per hundred NBR)	Compound N2	Compound N5
NBR (Nipol 1042)	100	100
Stearic acid	1	1
Zinc oxide	5	5
Sulfur	1.5	1.5
MBTS 2,2’-Benzothiazyl Disulfide	1.5	1.5
TMTD Bis(dimethylthiocarbamoyl) Disulfide	0.5	0.5

DOS	10	10
Carbon black (n330)		23
Silica (Nipsil VN3)		28
Density	1.015	1.182
Hardness (Shore A Durometer)	43.4	65.8

2.3 Compression set

Compression set tests were conducted both before hydrogen exposure and 30 min after exposure at hydrogen gas pressures up to 90 MPa for 22 h at 110°C. The dimensions of the specimens were first measured using a laser micrometer before they were placed on the bottom plate of the compression setup previously described in the work of Menon et al. [14] A constant deflection of 25% was applied to the specimens, with a 2.35 mm thick space bar in accordance with the ASTM standard D395, Method B. Then, the dimensions were measured with the laser micrometer after removal from the compression setup and given a 30 min recovery at room temperature. Compression-set ratios were calculated as a percentage of the original deflection using the equation below:

$$C_B = \left[\frac{(t_0 - t_1)}{(t_0 - t_n)}\right] \times 100\% \quad (1)$$

where C_B stands for compression set in percentage, t_0 for original thickness of the specimen, t_1 for final thickness of the specimen, and t_n for thickness of the spacer bar.

2.4 Helium-ion microscopy

Image analyses of surfaces and through-thickness fractures were performed using a Zeiss ORION PLUS helium-ion microscope (HeIM). The HeIM has a resolution of less than 0.3 nm at an energy of 25–30 kV and beam currents between 1 fA and 25 pA. Depending on the substrate material, the helium-ion beam produces 3–9 secondary electrons for each incoming helium ion. This creates a better signal and higher image contrast between different materials that is not seen with a traditional scanning electron microscope.

2.5 Chemical analysis

Time-of-flight secondary ion mass spectrometer (TOF-SIMS) measurements were performed using a TOF.SIMS 5 instrument (IONTOF GmbH, Münster, Germany) for chemical analysis. A 10 keV argon cluster beam was used to clean sample surfaces to remove contamination. The argon cluster beam was scanned over a 600 × 600 μm^2 area, and about 10–20 nm of material was removed before imaging analysis. A 25.0 keV Bi^{3+} beam was used as the analysis beam to collect SIMS images. The Bi^{3+} beam (~0.36 pA) was focused to ~400 nm in diameter and scanned over both a 500 × 500 μm^2 area and a 200 × 200 μm^2 area at the center of the argon cluster crater. The images were 512 × 512 pixels, and the total image collection time was about 500 s. A low-energy (10 eV) electron flood gun was used for charge compensation in all measurements.

2.6 High-pressure NMR experiments

High-pressure nuclear magnetic resonance (NMR) experiments were run on a 300-MHz Varian INOVA spectrometer using a 5 mm pencil style Chemagnetics HXY magic angle spinning probe. The rotors were the WHiMS [15] rotor design fitted with a check valve bushing to retain the gas in the rotor. After the rotors were filled with 50–60 mg of rubber, they were put into a pressure chamber and then held at the intended pressure for at least 10 min. The ^{1}H single pulse experiments used a 4 μs, 90-degree pulse, 5 s recycle delay, and 1 s acquisition time. The spinning speed for these experiments was 4 kHz.

2.7 Density tests

Density measurements were performed following the same method as used in the prior work of Menon et al. [14] Based on ASTM D792-13, the specimens were measured immediately after 90 MPa hydrogen exposure and 48 h after removal from the pressure vessel. Weights were determined in air using a Mettler Toledo XS403S balance with a repeatability of 0.5 mg ± 0.0008% gross weight of the specimen. The specimens were then immersed in deionized water using the designated setup and their apparent masses after immersion were determined. The water temperature, water density, and air density at 21°C were used to calculate density, using the following equation:

$$\boldsymbol{\rho = \left[\frac{(W_{air})}{(W_{air} - W_{water})}\right] \times (D_{water} - D_{air}) + D_{air}} \quad (\mathbf{2})$$

where $\boldsymbol{\rho}$ is the density of the specimen, $\boldsymbol{W_{air}}$ is the weight of the specimen in air at 21°C, $\boldsymbol{W_{water}}$ is the weight of the specimen in water at 21°C, $\boldsymbol{D_{water}}$ is the density of water at 21°C, and $\boldsymbol{D_{air}}$ is the density of air at 21°C.

2.8 Transmission electron microscopy

The material was dissected to 0.5 × 0.5 × 2 mm cuboids, mounted with 2.3% sucrose solution on specimen carriers (Leica Microsystems, #16701952), and flash-frozen in liquid nitrogen. Ultrathin sections (70 nm) were prepared using a Leica UC7 ultramicrotome operating at −120°C. They were collected on 100 mesh Cu grids coated with Formvar and carbon (Electron Microscopy Sciences) and imaged with a Tecnai T-12 TEM (FEI) operating at 120 kV with a LaB_6 filament. Images were collected digitally using a 2_2K UltraScan 1000 charge-coupled device camera (Gatan).

3.0 RESULTS AND DISCUSSION

Figure 2 illustrates both the effects of 90 MPa, high-pressure hydrogen at 110°C for 22 hours on the compression-set performance of NBR compounds N2 and N5 and the changes that occurred before and after hydrogen pressure exposure. N2 has plasticizer but no filler, while N5 has both filler and plasticizer. According to the results, N2 and N5 NBR materials increased in compression set by ~37% due to hydrogen exposure. The increase in compression set in both material systems was followed up with a series of analyses using a helium-ion microscope to evaluate the surface and fractured cross sections for changes in the material.

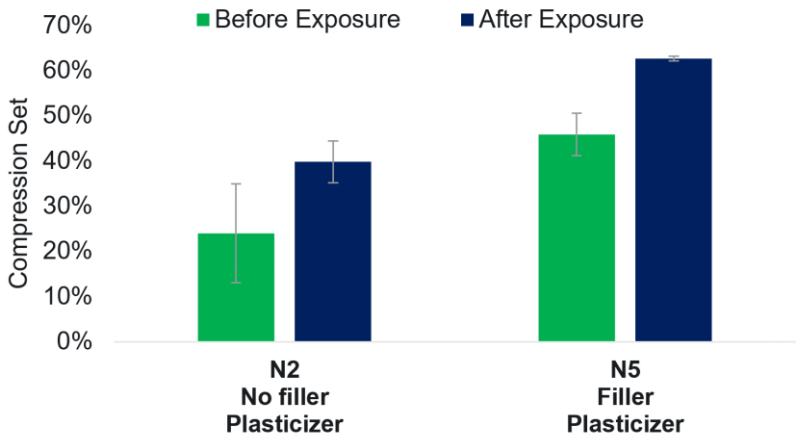

Figure 2. Effects of high-pressure hydrogen exposure on compression set.

Figure 3 shows surface morphology before and after the N2 rubber compound was exposed to 28 MPa hydrogen gas. In particular, prior to high-pressure hydrogen exposure, there were cracks about 1 μm wide on the surface with no sign of plasticizers, as shown in Figure 3(a) and (b). After being saturated in the 28 MPa hydrogen environment for 24 hours, the specimen developed a large number of circular, dark elements at the surface, with a few elliptical, dark elements along the edges of the crack (Figure 3(c) and (d)). The development of such dark elements is ascribed to the potential phase separation and plasticizer agglomeration in the presence of high-pressure hydrogen. It has been reasoned that plasticizer–plasticizer interaction is greater than rubber–plasticizer interaction [16] and that the introduction of hydrogen gas could initiate aggregation. Also, the breadth of the crack increased to about 1.3–1.4 μm, possibly due to swelling during gas decompression.

The N5 rubber compound was cryo-fractured in liquid nitrogen to form cross-sectional faces, which can provide useful information on the internal microstructure under the influence of high-pressure hydrogen. Figure 4(a) and (b) show the structure at the fractured face before and after hydrogen treatment, respectively. It is evident that phase separation and plasticizer aggregation occurred to a large extent during hydrogen exposure, consistent with the observations on the N2 specimens. It has been postulated that the hydrogen that diffused into the polymer could act as a solvent and thereby increase the mobility of plasticizers to promote aggregation. The obvious change in morphology shows an increase in dark regions (plasticizer phase) and reduction of the light regions (polymer phase). To further validate our theory, TOF-SIMS was used for chemical analysis. Results are shown in Figure 4, where nitrile groups (CN-) in the polymer are distinguished in green, and oxygens (O-) in red for the DOS plasticizer. Figure 4(c) clearly is in good agreement with observations from the HeIM images, revealing phase separation between the nitrile rubber matrix and DOS plasticizers.

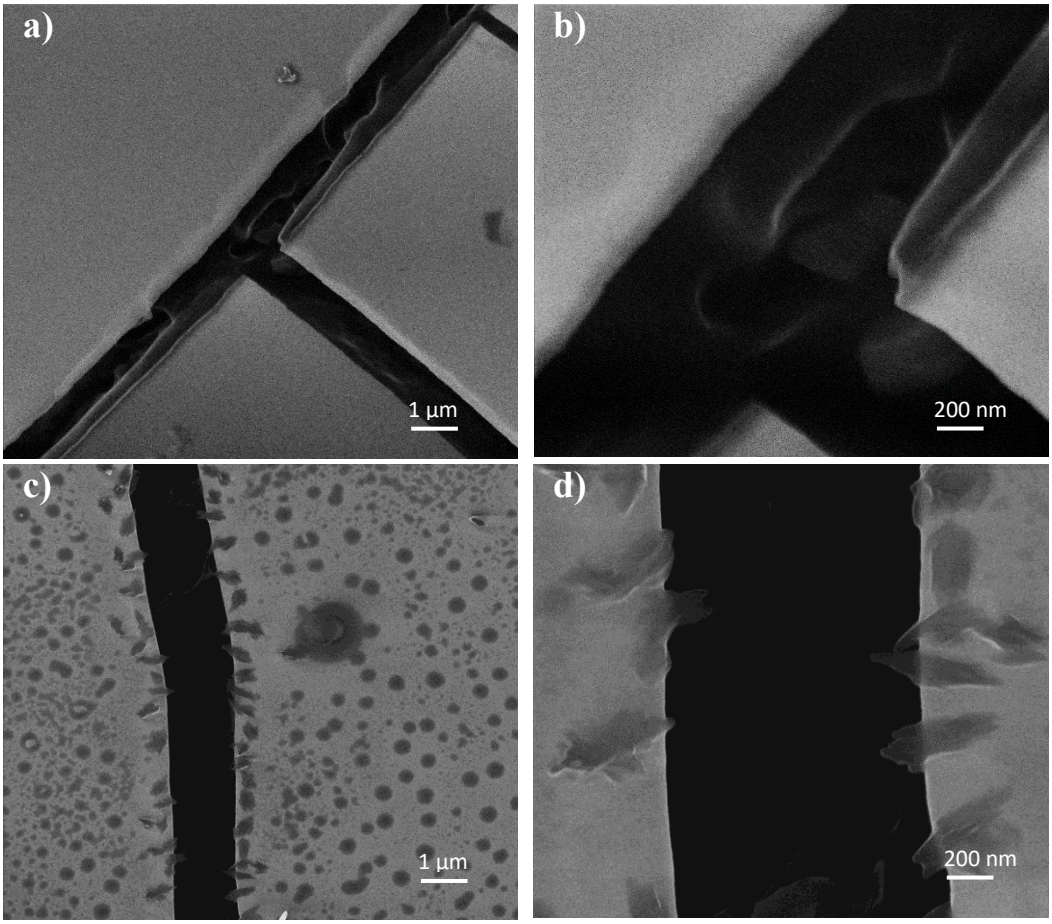

Figure 3. HeIM images of N2 surface morphology before (a and b) and after (c and d) 28 MPa hydrogen exposure.

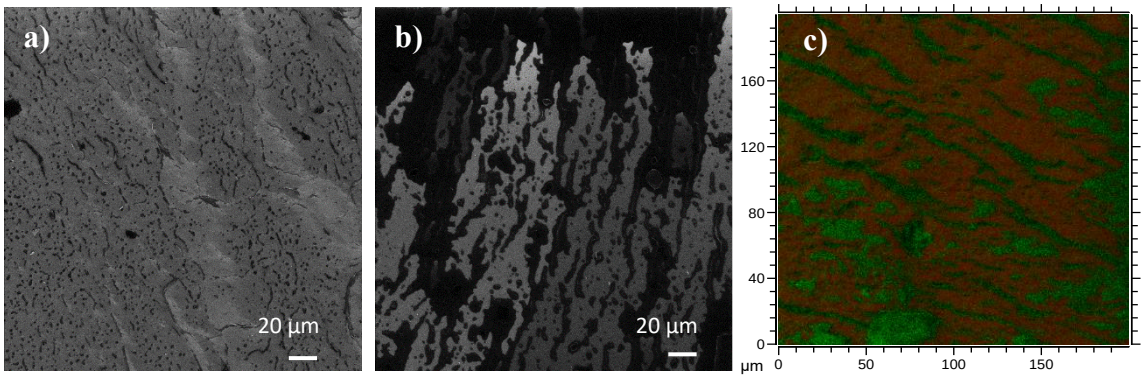

Figure 4. HeIM images of N5 cryo-fractured faces (a) before and (b) after 28 MPa hydrogen exposure; (c) TOF-SIMS analysis of N5 cryo-fractured face after exposure: CN- groups (green) and O- groups (red).

Another common observation was a volumetric change in samples after high-pressure hydrogen exposure in one static pressure cycle. As shown in Table 1, the percentage of volume swelling is significant in both NBR compounds. The unfilled, plasticized NBR compound, N2, swelled by as much as 85%, while the filled NBR compound, N5, underwent 13% less swelling. These large volumetric changes can induce damage within the interior of the material. As shown in Figure 1, the damage varies from material to material. Based on the observations in Figure 4 and Table 2, further investigation into the origin of hydrogen interaction within the material system was initiated.

Table 2. Volumetric change in material after 90 MPa, 24 hour hydrogen exposure.

Sample ID	Carbon/silica filler	Plasticizer	Percent increase in volume	Recovery in volume
N2	No	Yes	85%	97%
N5	Yes	Yes	72%	97%

It is well known that voids or process defects in materials are sites of gas accumulation and failure in elastomers. This research on NBR focused on where the hydrogen was moving within the material and how the filler may be influencing the gas mobility. Previous work by Shin Nishimura at Kyushu University's 2018 Hydrogenius conference on polymers [17] found that filler and plasticizer can change the diffusion coefficient of hydrogen in the materials. As shown in Figure 5, a series of NMR studies were able to identify hydrogen gas that had condensed within the unfilled, plasticized N2 material. The study used Pacific Northwest National Laboratory's (PNNL's) unique high-pressure gas rotor system, which can subject samples to up to 10 MPa of gas pressure during the experiment and then reduce the pressure back to ambient after analysis. The experiment looked at three different conditions. The first condition was baselining NBR N2 (Figure 5, top curve) in which no free or condensed hydrogen was found at 4.89 ppm or 5.3 ppm, respectively. The second experiment raised the internal hydrogen rotor pressure to 10 MPa to determine the amount of hydrogen moving into the material upon the first exposure to 10 MPa hydrogen. As shown in the bottom spectrum of Figure 5, a large free-hydrogen peak at 4.89 ppm and a small condensed-hydrogen peak at 5.3 ppm indicate gas diffusing into the polymer's pores. A third NMR experiment was performed in which the material was subjected to a high-pressure hydrogen exposure of 28 MPa and then analyzed in the NMR instrument under 10 MPa hydrogen rotor pressure. The results show an increase in the condensed-hydrogen peak, indicating an increase of condensed hydrogen in the pores.

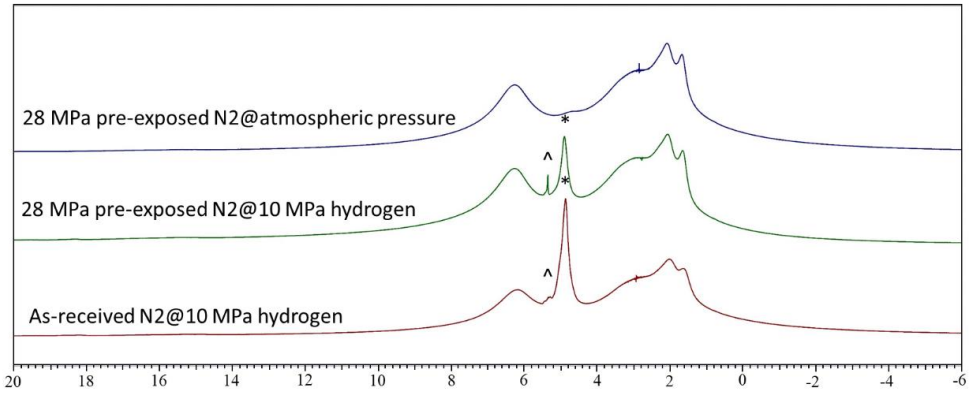

Figure 5. 1H-NMR spectra of N5 specimens prepared in various conditions. Pre-exposure to 28 MPa hydrogen was done in a high-pressure vessel, and in-situ NMR tests were run in a 10 MPa hydrogen environment. The peak at 4.89 ppm represents the free hydrogen (*), while that at 5.3 ppm indicates the hydrogen condensed with the material (^).

The NMR studies were followed up with a TEM analysis of specimens before and after high-pressure hydrogen exposure. Figure 6 shows a significant increase in the number of nanovoids initiated by hydrogen gas cavitation during gas decompression. The size and density of the voids were significantly increased after one pressure cycle. The number of voids increased by over five times that in the baseline image, as summarized in Table 3. The small inclusions after hydrogen treatment averaged 20 nm to 25 nm in length and 15 nm in width. However, the frequency of smaller inclusions was much more significant, and the size of the smaller inclusions was less than 10 nm. The inclusions could be the regions of free volume in the polymer where gas could condense.

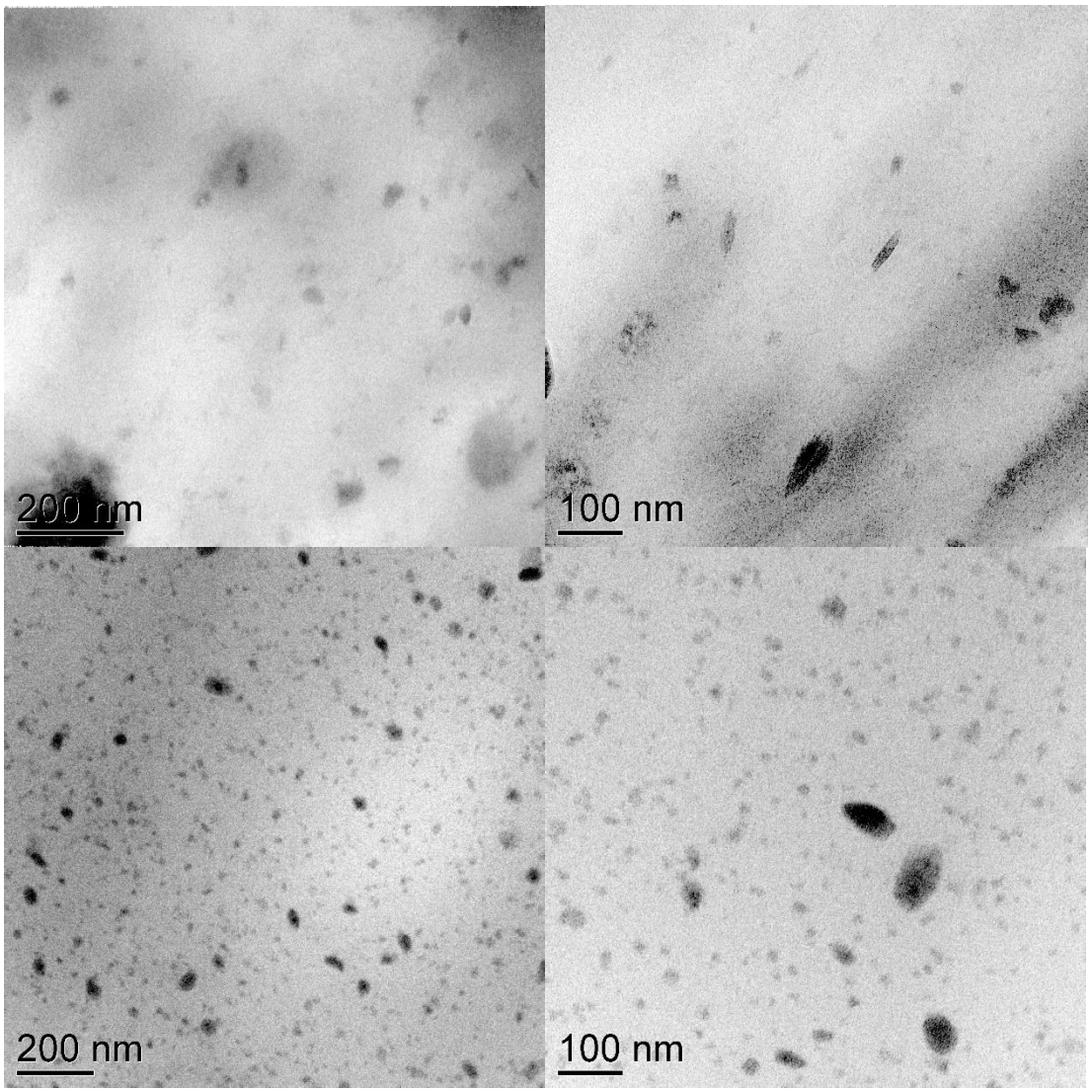

Figure 6. TEM images of N2 before exposure (top left: Pre-H_2 N2_1; top right: Pre-H_2 N2_2) and after exposure to 28 MPa hydrogen (bottom left: Post-H_2 N2_1; bottom right: Post-H_2 N2_2).

Table 3. TEM image analysis of void inclusions in Figure 6.

	Pre-H_2	**Pre-H_2**	**Post-H_2**	**Post-H_2**
Image ID	**N2_1**	**N2_2**	**N2_1**	**N2_2**
Scale bar	100 nm	200 nm	100 nm	200 nm
Particle counts	16	27	101	133
Area dimension (nm × nm)	718.5 × 718.5	1405.4 × 1405.4	718.5 × 718.5	1405.4 × 1405.4
Average length (nm)	41.1175	43.0833	25.1993	22.4759
Average width (nm)	20.5969	26.0111	15.154	14.4684
Length SD* (nm)	25.2545	16.6617	21.3542	10.1902
Width SD (nm)	8.3781	9.9572	6.5635	6.5694

* Standard deviation

4.0 CONCLUSIONS

Polymer materials play an important role in hydrogen infrastructure components by providing both static and dynamic sealing as well as high performance barrier. High-pressure hydrogen gas interaction with polymers is not

well understood in the hydrogen community. It is therefore of high importance to understand why each polymer system behaves differently on a submicron scale, which is less explored. With increased understanding of the influence of high-pressure hydrogen, future materials can be designed to improve the reliability and performance of the polymer systems. It is noted that elastomers have been sucessfully applied since decades in pressurized system in hydrogen industries and failures can be avoided by regular inspection and replacement. However, doing so adds significant expense and cost to operation of hydrogen infrastructure and causes frequent shutdown of services.

The composite nature of elastomer systems such as NBR adds other complexities to their material systems in formulating target properties for a specific application. One important property in elastomer formulation design is compression set in elastomeric O-rings for pressure systems. Compression set in NBR material compounds is significant, with nearly a 40% increase after high-pressure hydrogen exposure. The increase in compression set can reduce sealing performance and thus results in a loss of hydrogen, and in some cases affect the safety-level requirements of a facility, causing shutdowns and costly down time. Focusing on NBR rubber-material systems provides insight into how high-pressure hydrogen exposure can increase plasticizer mobility within the material. Increasing phase size distribution in the material can cause a change in material property performance and even plasticizer loss, with plasticizer blooming to the surface of the material.

It is well known and widely observed that some polymer systems increase in volume more than others. The model NBR compound studied demonstrated a 72–85% increase in volume. NMR studies show the hydrogen content increases with high-pressure exposure and condenses into the pores of the polymer. TEM analysis shows an increase in nanovoids in the polymer after exposure to 28 MPa high-pressure hydrogen. These small, nanosized voids were observed after one pressure cycle and are the nucleus for large void formation and gas permeation over time.

ACKNOWLEDGEMENTS

We gratefully acknowledge the financial support of the U.S. Department of Energy (DOE) under Contract No. DE-AC05-76RL01830. We also acknowledge support from the Environmental Molecular Sciences Laboratory (EMSL). EMSL is a national scientific user facility sponsored by the Department of Energy's Office of Science, Biological and Environmental Research program that is located at Pacific Northwest National Laboratory.

DISCLAIMER

The views and opinions of the authors expressed herein do not necessarily state or reflect those of the United States Government or any agency thereof. Neither the United States Government nor any agency thereof, nor any of their employees, makes any warranty, expressed or implied, or assumes any legal liability or responsibility for the accuracy, completeness, or usefulness of any information, apparatus, product, or process disclosed, or represents that its use would not infringe privately owned rights.

REFERENCES

1. Schlapbach, L. and Züttel, A., Hydrogen-Storage Materials for Mobile Applications, *Nature*, **414**, 2002, pp. 353-358.
2. Eberle, U., Müller, B., and von Helmolt, R., Fuel Cell Electric Vehicles and Hydrogen Infrastructure: Status 2012, *Energy & Environmental Science*, **5**, 2012, pp. 8780-8798.
3. Jain, I. P., Hydrogen the Fuel for 21st Century, *International Journal of Hydrogen Energy*, **34**, 2009, pp. 7368-7378.
4. Schlapbach, L., Hydrogen-Fueled Vehicles, *Nature*, **460**, 2009, pp. 809-811.
5. Woodtli, J. and Kieselbach, R., Damage Due to Hydrogen Embrittlement and Stress Corrosion Cracking, *Engineering Failure Analysis*, **7**, No. 6, 2000, pp. 427-450.
6. Djukic, M. B., Sijacki Zeravcic, V., Bakic, G. M., Sedmak, A., and Ragjicic, B., Hydrogen Damage of Steels: A Case Study and Hydrogen Embrittlement Model, *Engineering Failure Analysis*, **58**, pt.2, 2015, pp. 485-498.
7. Alvine, K. J., Shutthanandan, V., Arey, B. W., Wang, C., Bennett, W. D., and Pitman, S. G., Pb Nanowire Formation on Al/Lead Zirconate Titanate Surfaces in High-Pressure Hydrogen, *Journal of Applied Physics*, **112**, 2012, 013533.

8. Madina, V., Azkarate, I., Compatibility of Materials with Hydrogen. Particular Case: Hydrogen Embrittlement of Titanium Alloys, *Internation Journal of Hydrogen Energy*, **34**, 2009, pp. 5976-5980.

9. Jaravel, J., Castagnet, S., Grandidier, J., and Benoit, G., On Key Parameters Influencing Cavitation Damage upon Fast Decompression in a Hydrogen Saturated Elastomer, *Polymer Testing*, **30**, No. 8, 2011, pp. 811-818.

10. Schrittesser, B., Pinter, G., Schwarz, Th., Kadar, Z., and Nagy, T., Rapid Gas Decompression Performance of Elastomers – A Study of Influencing Testing Parameters, *Procedia Structural Integrity*, **2**, 2016, pp. 1746-1754.

11. Koga, A., Uchida, K., Yamabe, J. Nishimura, S., Evaluation on High-Pressure Hydrogen Decompression Failure of Rubber O-ring Using Design of Experiments, *International Journal of Automotive Engineering*, **2**, 2011, pp. 123-129.

12. Fujiwara, H., Ono, H., and Nishimura, S., Degradation Behavior of Acrylonitrile Butadiene Rubber After Cyclic High-Pressure Hydrogen Exposure, *International Journal of Hydrogen Energy*, **40**, No. 4, 2015, pp. 2025-2034.

13. Ohyama, K., Fujiwara, H., Nishimura, S., Inhomogeneity in Acrylonitrile Butadiene Rubber during Hydrogen Elimination Investigated by Small-Angle X-ray Scattering, *International Journal of Hydrogen Energy*, **43**, 2018, 1012-1024.

14. Menon, N. C., Kruizenga, A. M., Alvine, K. J., San Marchi, C., Nissen, A., Behaviour of Polymers in High Pressure Environments as Applicable to the Hydrogen Infrastructure, Proceedings of the ASME 2016 Pressure Vessels and Piping Conference, 17-21 July 2016, Vancouver, BC, Canada.

15. Walter, E.D., Qi, L., Chamas, A., Mehta, H.S., Sears, J.A., Scott, S.L., Hoyt, D.W., *Operando* MAS-NMR Reaction Studies at High Temperatures and Pressures, *J. Phys. Chem. C*, **122**, No. 15, 2018, pp. 8209-8215.

16. Lawandy, S. N., Halim, S. F., Darwish, N. A., Structure Aggregation of Carbon Black in Ethylene-Propylene Diene Polymer, *eXPRESS Polymer Letters*, **3**, No. 3, 2009, 152-158.

17. Nishimura, S., Polymeric Materials for Hydrogen Devices, International Symposium of Hydrogen Polymers Team, Hydrogenius, 2 February 2018, Kyushu University, Japan.